Optical Engineering

SPIEDigitalLibrary.org/oe

Mobile speckle interferometer in the long-wave infrared for aeronautical nondestructive testing in field conditions

Jean-François Vandenrijt
Cédric Thizy
Igor Alexeenko
Giancarlo Pedrini
Jonathan Rochet
Birgit Vollheim
Iagoba Jorge
Pablo Venegas
Ion López
Wolfgang Osten
Marc P. Georges

SPIE

Mobile speckle interferometer in the long-wave infrared for aeronautical nondestructive testing in field conditions

Jean-François Vandenrijt
Cédric Thizy
Université de Liège
Centre Spatial de Liège
Avenue du Pré Aily, Angleur (Liège), Belgium

Igor Alexeenko
Universität Stuttgart
Institut für Technische Optik
Pfaffenwaldring 9, Stuttgart, Germany
and
Immanuel Kant Baltic Federal University
Kaliningrad, A. Nevskogo str. 14, Russia

Giancarlo Pedrini
Universität Stuttgart
Institut für Technische Optik
Pfaffenwaldring 9, Stuttgart, Germany

Jonathan Rochet
Optrion
Pôle d'Ingénierie des Matériaux de Wallonie
Boulevard de Colonster 4, Liège, Belgium

Birgit Vollheim
InfraTec GmbH
Gostritzer Str. 61–63, Dresden, Germany

Iagoba Jorge
Pablo Venegas
Ion López
Centro de Tecnologías Aeronáuticas
Parque Tecnológico de Álava
C/Juan de la Cierva 1
Miñano (Álava), Spain

Wolfgang Osten
Universität Stuttgart
Institut für Technische Optik
Pfaffenwaldring 9, Stuttgart, Germany

Marc P. Georges
Université de Liège
Centre Spatial de Liège
Avenue du Pré Aily, Angleur (Liège), Belgium
E-mail: mgeorges@ulg.ac.be

Abstract. We present the development of a speckle interferometer based on a CO_2 laser and using a thermal infrared camera based on an uncooled microbolometer array. It is intended to be used for monitoring deformations as well as detecting flaws in aeronautical composites, with a smaller sensitivity to displacement compared to an equivalent system using visible (VIS) lasers. Moreover the long wavelength allows working with such interferometers outside the laboratory. A mobile system has been developed on the basis of previous laboratory developments. Then it is validated in a variety of industrial nondestructive testing applications in field working conditions. [DOI: 10.1117/1.OE.52.10.101903]

Subject terms: speckle interferometry; speckle metrology; long-wave infrared; microbolometer arrays; CO_2 lasers; nondestructive testing; composites.

Paper 130168SS received Feb. 1, 2013; revised manuscript received Mar. 5, 2013; accepted for publication Mar. 6, 2013; published online Apr. 11, 2013.

1 Introduction

Methods based on holographic interferometry (HI)[1] and electronic speckle pattern interferometry (ESPI)[2] are commonly used for nondestructive testing (NDT) of mechanical structures and dynamic analysis. These techniques are based on the comparison of wavefronts recorded at different instants. The result of the wavefronts comparison is the phase difference containing information about the object displacement field during the recording. There are many publications describing results obtained by HI and ESPI using visible (VIS) or ultraviolet light; however, few investigations in long-wave infrared (LWIR) spectral range (corresponding to CO_2 lasers) were realized up to now.

The interest in using longer wavelengths for such interferometric technique is in two areas. On one hand, the longer

wavelength allows the displacement measurement range to be increased, which can be an advantage compared to VIS-wavelength HI or ESPI, which allow measurement ranged between a few tenths of a micrometer up to a few micrometers, depending on the number of resolvable fringes in the interferograms (function of pixel number and noise). In the case of CO_2 lasers, the 10.6-μm wavelength allows a measurement range that is 20 times larger than with VIS systems. On the other hand, the local interference of reference and object beams, which form the hologram in HI or the specklegram in ESPI, has to be stable during the recording time. One generally considers that the two recording beams cannot move between one another by a tenth of wavelength. For this reason, a holography or ESPI setup is generally confined to laboratories or quiet conditions when VIS wavelengths are considered.

In the past, some groups have worked on photochemical materials for LWIR hologram recording and some of which applied them to HI. A review of these works can be found in Ref. 3. Løkberg and Kwon[4] were the first to propose ESPI with a CO_2 laser and recording on a pyroelectric vidicon camera. This technology is sensitive to variations of light intensity; therefore, their experiments were limited to vibrating objects. Digital holography (DH) with electronic hologram recording and numerical reconstruction was proposed[5,6] with modern pyroelectric modified camera (no longer requiring intensity variations) in the Mach-Zehnder configuration for reconstructing small object images. The microbolometer array camera technology was then demonstrated in DH by George et al.[7] in a similar configuration. Since then, many works followed in the area of applying microbolometer arrays to observations of large objects by DH.[8–10] One advantage of LWIR in DH is that the ratio between the wavelength and the pixel size is larger than in the VIS spectral range. Since this ratio directly affects the observable object size, LWIR DH allows the reconstruction of objects that are typically 5 to 10 times larger than in VIS.[3,9,10]

Vandenrijt and Georges showed the use of an uncooled microbolometer camera (sensitive in the 8 to 14 μm range) with medium lateral resolution (320×256 pixels) in various setups such as in-plane ESPI,[11,12] out-of-plane ESPI,[12] and lensless digital HI.[12] These works were oriented toward optical metrology, and we applied phase shifting to ESPI for obtaining quantitative displacements that were compared to another measurement technique. We discussed specific aspects related to the use of LWIR, including the fact that an object with a given roughness shows a higher specular reflection in LWIR than in VIS. Following Yamaguchi,[13] the surface becomes completely scattering, and speckle appears when the laser wavelength is smaller than the surface roughness. On the other hand, specular reflection appears as soon as the wavelength is larger than the roughness, and it quickly dominates the speckle pattern intensity. This problem was tackled by using a removable scattering powder, which increases the roughness in such a way that speckles appear and allow application of ESPI.[12]

These preliminary works were followed by two separate projects. The first consists of the development of LWIR digital holographic interferometry (DHI) for monitoring the deformation of large-space aspheric reflectors in thermal-vacuum testing, reproducing the conditions undergone by these structures when in orbit. In these cases, the objects have a small roughness and already appear specular in VIS. For many reasons explained in Ref. 3, they cannot be covered by scattering powder. Therefore, we developed a specific diffuse illumination in the LWIR for producing virtual speckles onto the observed surface.[3]

The second project is related to NDT of aeronautical composites. Usually they are made of carbon-fiber-reinforced plastics (CFRP), and in less proportion of glass-fiber-reinforced plastics (GFRP) or Kevlar. In a first paper on that topic, we showed that the natural roughness of such materials was high enough to generate speckles.[14] We then presented various interferometric techniques such as LWIR off-axis DHI,[15,16] out-of-plane ESPI[16] and shearography.[16] In Ref. 16, we presented in detail the development of the interferometric configuration, especially the combination between the reference and object beams inside the thermal camera, because of some specific aspects related to the objective lens that cannot be detached from the camera head. In these studies, a high-resolution microbolometer camera was used, with 640×480 pixels (VarioCAM hr; Jenoptik, Jena, Germany). This state-of-the-art camera allowed a further expansion of the quality of the results compared to Ref. 12, and excellent-quality interferograms were demonstrated for detecting flaws inside various composite samples.

This paper presents a follow-up activity to what was shown in Ref. 16. In Sec. 2, we recall some basics of the out-of-plane ESPI in the LWIR. In Sec. 3, we present the development of a mobile system that is devoted to demonstrating the applicability of LWIR ESPI in field NDT applications. In Sec. 4, we present various NDT experiments that were carried out in realistic industrial conditions.

2 Basic Technique: Speckle Interferometry with a CO_2 Laser and Microbolometer Array

We will briefly recall some basics of ESPI and then explain the specific features of LWIR operations. ESPI consists of illuminating a diffusive object with a laser and superposing its image onto a camera detector with a reference beam coming directly from the laser. Expressed mathematically, the object beam on the detector array can be represented by its complex amplitude:

$$\boldsymbol{U}(x,y) = \boldsymbol{e_U}\sqrt{I_U(x,y)}\exp[i\varphi_U(x,y)], \tag{1}$$

where $I_U(x,y)$ is the wave intensity, $\varphi_U(x,y)$ the phase, and $\boldsymbol{e_U}$ the unit vector giving the wave polarization orientation. Similarly, the reference beam is given by

$$\boldsymbol{R}(x,y) = \boldsymbol{e_R}\sqrt{I_R(x,y)}\exp[i\varphi_R(x,y)]. \tag{2}$$

Their interference on the detector produces an intensity pattern $I(x,y)$ (specklegram) given by

$$I(x,y) = I_R(x,y) + I_U(x,y) + 2(\boldsymbol{e_R}\cdot\boldsymbol{e_U}) \times \sqrt{I_R(x,y)I_U(x,y)}\cos[\phi(x,y)], \tag{3}$$

where the relative phase difference between the object and reference waves is defined by $\phi(x,y) = \varphi_R(x,y) - \varphi_U(x,y)$. The contrast of interference $m(x,y)=(\boldsymbol{e_R}\cdot\boldsymbol{e_U})2\sqrt{I_R(x,y)I_U(x,y)}/[I_R(x,y)+I_U(x,y)]$ is maximized when the polarizations are

parallel ($\boldsymbol{e_R} \cdot \boldsymbol{e_U} = 1$) and when the beam intensities are equal [$I_R(x,y) = I_U(x,y)$].

In Ref. 16, we presented in detail various optical configurations of such interferometric technique. Particular attention was paid to the injection of the reference beam into the LWIR camera. One constraint with LWIR cameras is that the aperture stop is usually outside the objective lens, between the last lens and the detector. Moreover, a germanium window is always present in front of the microbolometer array. Finally, the used camera is equipped with a rotating aperture wheel, which allows radiometric calibration when used for thermography. As a consequence, it is not possible to insert a small beam combiner between the last lens of the objective and the detector array. The only choice we have is to inject the reference from the front of the objective lens. Several possibilities exist, and we analyzed the pros and cons of each in Ref. 16. Figure 1 shows the setup that was chosen from various configurations. We found that the best choice for reference beam injection was to use a beam combiner (BC) in front of the objective lens (OL). A reference lens (RL) expands the size of the reference beam in order to cover the whole detector array. In Ref. 16, we tried several beamsplitters (BSs) with various ratios R%/T%, where R% and T% are the reflected and transmitted percentages of the incident light power, respectively. The first is a R50/T50 BS from ULO Optics (Stevenage, England). Since the amount of light scattered by the object is low, a R50/T50 BS produces on the camera an object beam that is weak compared to the reference, and thus an attenuator (A) is required to balance the beams ratio and increase the contrast. The attenuator consists of two polarizers where the transmission axes are rotated with respect to each other. The output polarizer is also used for correctly orienting the polarization of the beams. The second possibility is to consider asymmetric ratio BS: R90/T10 or R99/T1 (manufactured by II–VI Company, Saxonburg, Pennsylvania) yielding an intrinsically small reference beam intensity, which better matches the scattered object beam intensity. However, it is still too high and requires a fine adjustment for beam ratio closer to unity. For that purpose, we use a polarizer (P) in the reference beam, which allows for adjusting its intensity, the laser beam being polarized. Despite the fact that the polarization direction of the reference beam is changed ($\boldsymbol{e_R} \cdot \boldsymbol{e_U} < 1$), the polarizer transmission direction is very close to the laser polarization. However, this has little influence on the final interference contrast.

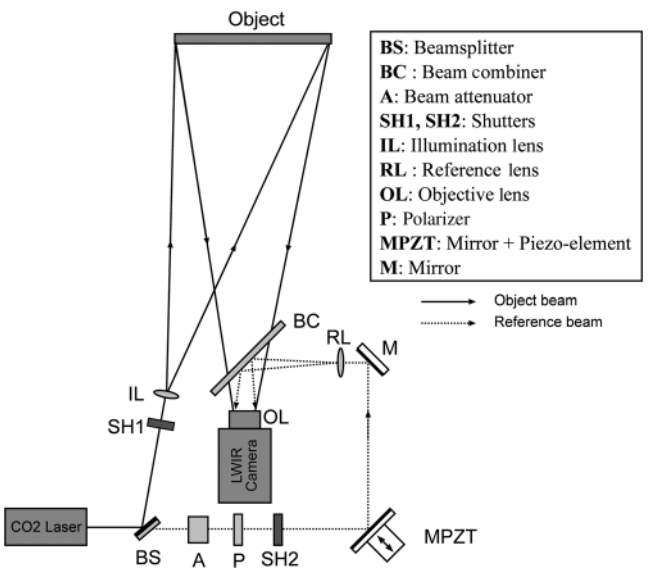

Fig. 1 Scheme of LWIR out-of-plane ESPI laboratory setup.

During the acquisition of the specklegrams, the camera is synchronized with the phase shifting of the piezo element: Four specklegrams are recorded at four positions of the MPZT mirror, which induce a $\lambda/2$ phase shift between each acquisition. Therefore, the phase-shifted specklegrams are expressed as

$$I_n = I_R + I_U + 2(\boldsymbol{e_R} \cdot \boldsymbol{e_U})\sqrt{I_R I_U}\cos\left(\phi + n\frac{\pi}{2}\right), \tag{4}$$

with $n = 1,2,3,4$. [The (x,y) dependency is left aside for simplicity.] Equation (4) is used to calculate the phase according to the well-known four buckets algorithm:

$$\phi = \tan^{-1}[(I_4 - I_2)/(I_1 - I_3)]. \tag{5}$$

If we record two such sets of four specklegrams $I_{n,a}$ and $I_{n,b}$ for two states of the object, noted a and b, one can compute their phases ϕ_a and ϕ_b. The phase difference $\Delta\phi = \phi_a - \phi_b$ can be related to the displacement $\boldsymbol{d}$ of each object point, imaged on each pixel of the camera (x,y). This relationship is given by

$$\Delta\phi = \frac{2\pi}{\lambda}\boldsymbol{s} \cdot \boldsymbol{d}, \tag{6}$$

where the sensitivity vector defined by $\boldsymbol{s} = \boldsymbol{k_1} - \boldsymbol{k_2}$ is determined by the geometry of the setup, with $\boldsymbol{k_1}$ and $\boldsymbol{k_2}$ the unit vectors of illumination and observation, respectively.

Here, with a single illumination almost collinear to the observation direction, the sensitivity vector lies globally along the observation direction. If the object is perpendicular to the latter, the out-of-plane displacement $d_\perp$ component is measured, and Eq. (6) reduces to $\Delta\phi = \frac{4\pi}{\lambda}d_\perp$.

3 Development of the Mobile System

A compact and transportable system was designed to be able to work outside the laboratory, in field conditions. Several scenarios were envisaged, and we discuss them next.

The first consists of using a remote CO_2 laser and a mobile head comprising the interferometric assembly and the thermal camera. The CO_2 laser was set in a rack including all electric supplies, as well as the water cooler regulating the temperature of the laser head. In such a case, the laser beam should be brought to the optical head through either a telescopic arm with folding mirrors inside it or an optical fiber. We rejected the telescopic arm because of the complexity for moving the optical head. Therefore, we made some investigations with multimode optical fibers working in the LWIR. We considered several optical fiber types working in the LWIR: hollow silica waveguides (300- and 500-μm core diameter) manufactured by Polymicro Technologies (Phoenix, Arizona), polycrystalline infrared (PIR) fibers (500-μm core diameter) manufactured by A.R.T. Photonics GmbH (Berlin, Germany), and chalcogenide glass fibers (100-μm core diameter) manufactured by Amorphous Materials Inc. (Garland, Texas). For all of them, we measured the transmission.

Hollow silica fibers allow 50% transmission for a 2-meter-long fiber and input power of 1 W. The coupling of the laser beam into the fiber was quite easy; however, a curvature radius of the fiber smaller than 20 cm yielded loss in the transmission and damaged the fiber cladding. Therefore, we rejected this fiber since it induces a practical constraint on the curvature radius. The PIR fiber showed a transmission of 60% for a 1-meter-long fiber and power of 1 W. It is easy to adjust as well through Sub Miniature Type A connectors (SMA) connectors and fiber couplers provided by the manufacturer. According to the specification, this kind of fiber could carry up to 20 W without damage. However, the admissible curvature radius is 20 centimeters, which is not suitable for our purpose. Finally, the chalcogenide fiber, which has a smaller core diameter, is very flexible and has a curvature radius on the order of a few centimeters. We measured 40% of transmission for a power of 100 mW. This fiber is made of soft material and higher powers can cause the fiber to melt. Therefore, they are not suited to transport high powers. Our conclusion was that for all the abovementioned reasons, the use of LWIR optical fibers was not suited to bring a laser beam from the laser to a remote optical head.

The second scenario was to place the CO_2 laser in the optical head. The laser was a compact Merit-S manufactured by Access Laser Co. (Everett, Washington). We selected a model emitting 8 W at 9.3 μm instead of using the 10.6-μm emission line. The choice of the 9.3-μm line was guided by the following considerations. In the project, the development of a LWIR camera with a cooled detector array was performed for better awaited performances than an uncooled camera. Main cooled detector technologies are quantum well infrared photodetector (QWIP) and IR photodiodes, mostly based on mercury cadmium telluride (MCT) alloys ($Hg_{1-x}Cd_xTe$).[17] These various technologies allow for better signal-to-noise ratios and higher frame rates than the uncooled microbolometer arrays. Nevertheless, their spectral response is usually limited to smaller ranges than microbolometer arrays, which cover the 8 to 14-μm range. In particular, the small spectral response band covered by a QWIP detector array has to be tailored to correspond to one of the emission lines of the CO_2 lasers.[17] The MCT detector arrays allow larger bands but with common cut-off wavelengths of around 10 μm.[17] Therefore, in view of using a LWIR camera based on the MCT technology, we envisioned using a 9.3-μm laser instead of 10.6 μm. At this step, the camera made available for our experiments showed tiny vibrations along the optical axis due to the sterling cooler. These vibrations are not relevant for thermography purposes; however, they negatively affect the ability to record speckleograms, even at our wavelengths. For these reasons, we considered in the mobile ESPI system the same camera as the one already used in the laboratory setup; i.e., the VarioCAM hr from Jenoptik, with 640×480 pixels.

Figure 2 presents the mobile setup, which is constituted of two main parts. The lower bench [Fig. 2(a)] incorporated the Merit-S CO_2 laser, a general shutter (SH), some folding mirrors (M1, M2, M3), a polarizing beamsplitter (PBS), and a half-wave plate (HWP). The PBS (manufactured by II-VI Company) consisted of two stacks of three ZnSe plates each and working at the Brewster angle, as shown in Fig. 2(b). Both stacks were placed in a chevron geometry, which allowed the transmitted beam to be collinear with the input beam, coming from M2. The extinction ratio of an arrangement with six plates was 500:1. The beam transmitted by the PBS carried the p-polarization and was the object beam (OB). It traveled up to the object through a periscope (M3-M4) and was enlarged by a lens (IL). The beam reflected by the PBS (dotted line) was s-polarized and constituted the reference beam (RB). The HWP (manufactured by II-VI Company) allowed for rotating the polarization of the laser beam before entering the PBS and then adjusting the beam ratio between the RB and OB at the level of the camera.

The upper bench of the setup [Fig. 2(c)] was placed just on top of the lower one, as shown in Fig. 2(a). The RB originating from the PBS in the lower bench reached the upper bench through a hole in the bench and reached the lens L. The spherical beam was then folded by a mirror mounted on a piezo-translator. The latter was used for inducing shifts of phase necessary for the phase-shifting technique. The RB is transmitted by a beam combiner (BC), and at first it was reflected back by a concave mirror (CM) and again by the BC toward the microbolometer array through the objective lens (OL) of the camera. The CM, with a diameter of 127 mm and a focal length of 102 mm, was made of Pyrex with a protected gold coating that had a reflectivity $R_{CM} = 0.98$ at 9.3 μm. The OL was made of germanium

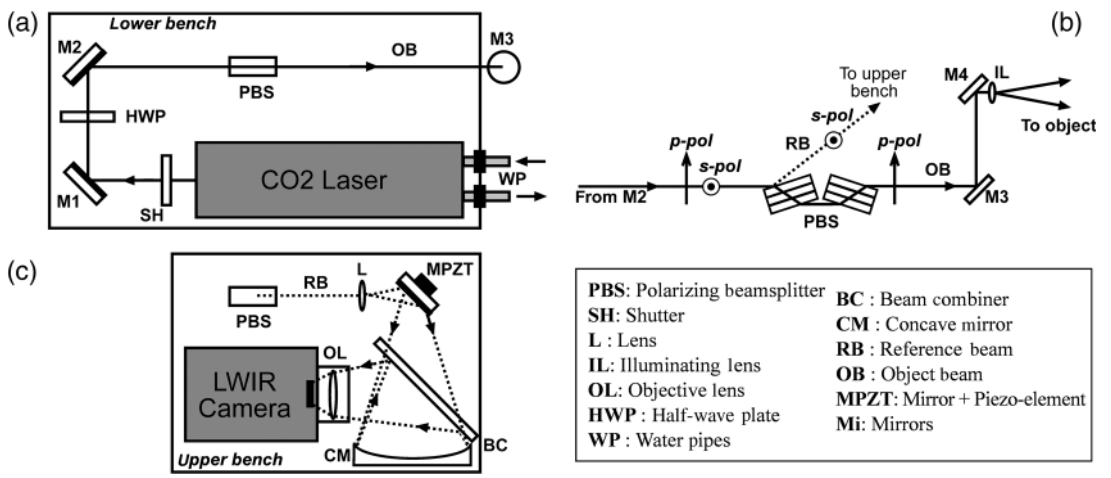

Fig. 2 Scheme of principle of the mobile LWIR speckle interferometer: (a) lower bench, (b) separation of beams in the lower bench, and (c) upper bench.

and had a focal length of 50 mm. It observed the object through the BC. The BC was not the same as the one used for the laboratory studies.[16] The one used here had transmittances for p- and s-polarizations of $T_p = 0.99$ and $T_s = 0.93$ at 9.3 μm, and reflectances $R_p = 0.05$ and $R_s = 0.055$, respectively. Therefore, most of the light backscattered by the object illuminated by OB through IL was transmitted through BC and reached the camera. From the power P of RB reflected by PBS, only $T_s.R_s.R_{CM} = 0.05\ P$ was directed toward OL.

Figure 3 shows a picture of the mobile LWIR ESPI system. Input and output water pipes (WPs) can be seen under the aperture by which the camera observes the object. The periscope is VIS on the right side of the front panel. WPs are shown short-circuited, but normally they are connected to the cooling system located in a mobile service cabinet, which also includes all power supplies for the laser, the camera and other optomechanical components of the bench. The ensemble of the hardware and software operations are controlled by LabVIEW (National Instruments Corporation, Austin, Texas) installed on a laptop.

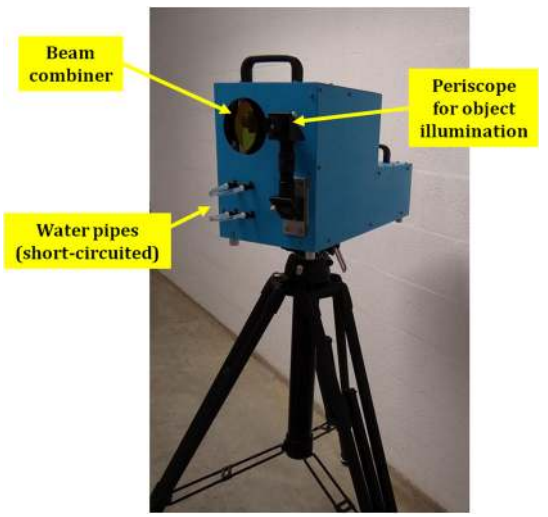

Fig. 3 Picture of the mobile LWIR speckle interferometer.

4 Industrial Applications

4.1 *Deformation Measurements in Structural Testing Facilities*

A series of demonstration tests were performed at the Centro de Tecnologías Aeronáuticas (CTA) in Miñano, Spain. Several structural testing facilities were running in large hangars and the mechanical behavior of aeronautics structures were analyzed under various loading conditions. A first test was the observation of dynamic deformation of a composite panel in a tensile test machine (Fig. 4). The object was a monolithic CFRP (31 cm wide and 41 cm high), but the observed area (shown by red dotted lines) was typically 25×19 cm^2. The tensile machine allows elongation of specimen in the vertical direction (red arrow), thus mainly producing in-plane deformations. Nevertheless, out-of-plane displacements arose for high loads, and they could be measured by our instrument. Figure 5 shows phase maps $\Delta\phi$ at several load conditions during a cycle applied to the specimen shown in Fig. 4. The clamping of the plate to the tensile

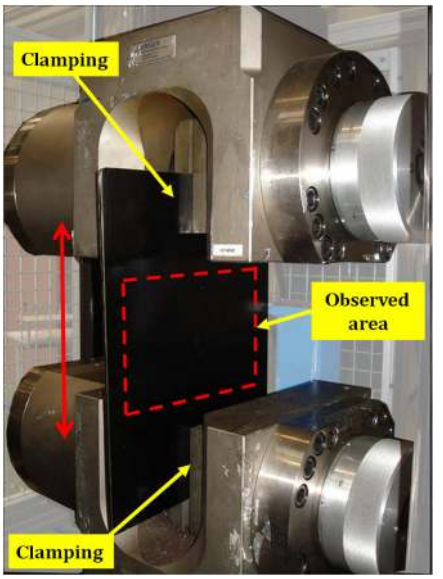

Fig. 4 Tensile test machine with composite plate.

machine is on the left and right sides of the images, and the red arrow shows the direction of the traction.

Figure 6 shows a second test being performed at CTA on a helicopter tailboom (typically 4 meters long and clamped at one side), while a vertical hydraulic actuator attached at the other side allowed the free edge to be displaced by a few centimeters. This test rig was placed in a large hangar

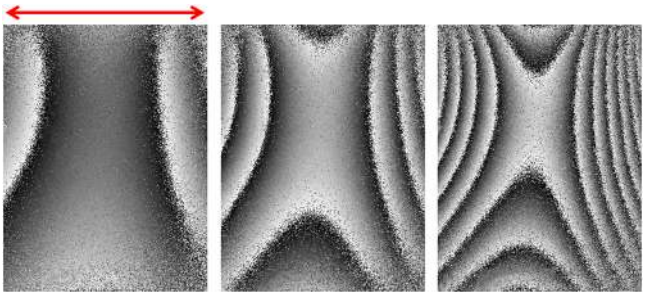

Fig. 5 Phase maps corresponding to increasing load conditions in the tensile tests during a cycle. The red arrow shows the direction of the elongation.

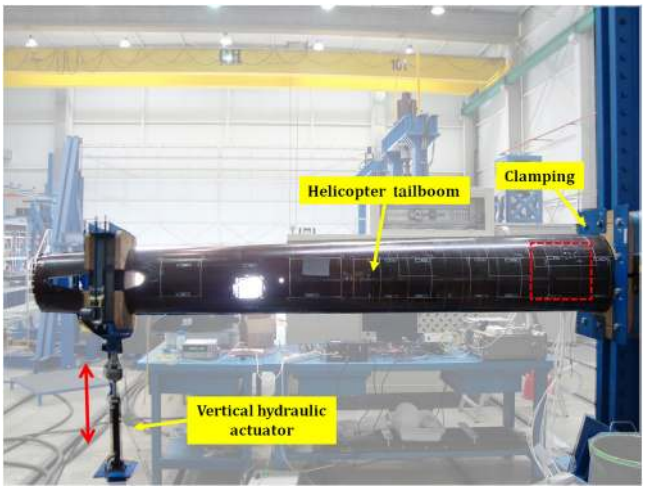

Fig. 6 Test rig for mechanical actuation of a helicopter tailboom.

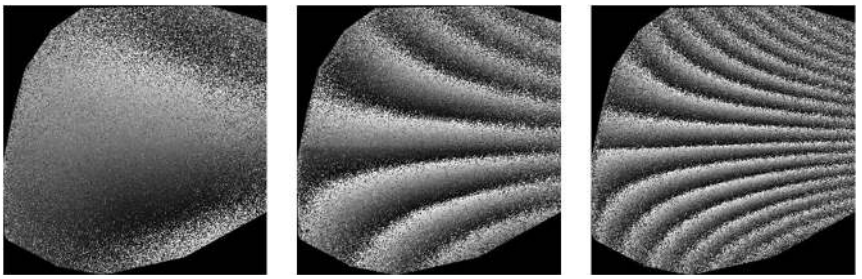

Fig. 7 Phase maps showing the tailboom deformation at different instants during a load cycle.

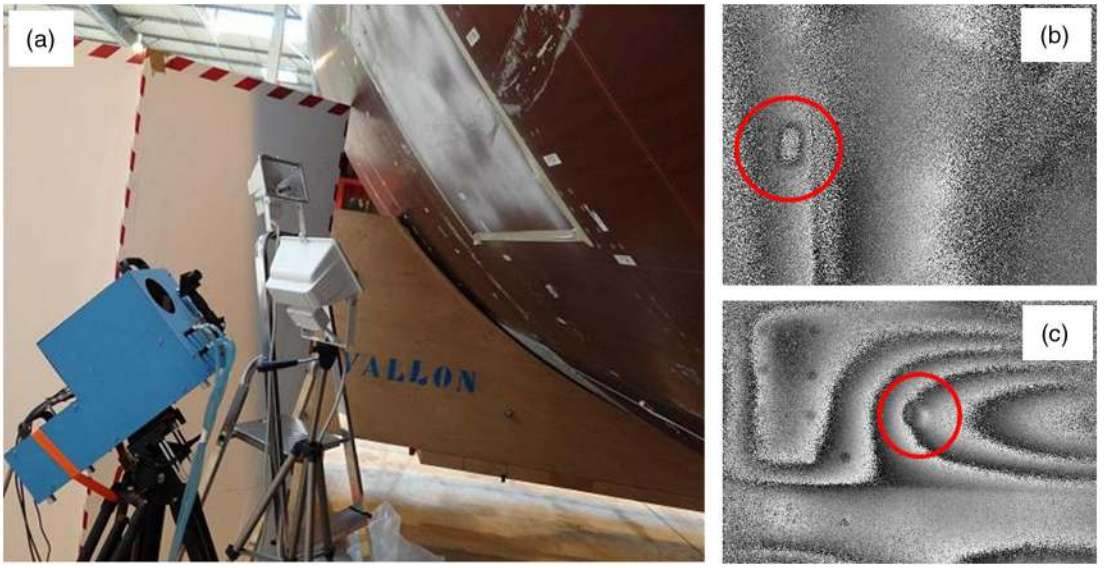

Fig. 8 (a) The mobile LWIR ESPI instrument in front of a large composite structure in the testing area. (b) and (c) Various defects detected after thermal loading with halogen lamps.

with other test rigs working at the same time as our experiments with operators around. Our instrument was placed to observe the area surrounded by the red dotted lines close to the clamping point. It must be mentioned that Fig. 6 shows the convex external part of the specimen, while we observed this zone from the internal concave side. It must be noted that a white removable powder similar to the one discussed in Refs. 12 and 16 has been applied to the specimen because some of its parts were too specular and backreflections of the laser beam could have damaged the microbolometer array.

Figure 7 shows phase maps obtained by loading of the tailboom at different instants of a load cycle. While the mechanical solicitation is applied mainly vertically, the important curvature of the tailboom induces strong out-of-plane deformation close to the clamping zone. In Fig. 7 the clamping is located on the left side of the pictures and the actuator is far to the right (out of the observed field). We have not compared these measurements to those obtained by other techniques. However, the aim of this experiment was to analyze the ability of the detector to provide exploitable interferograms during measurements in field conditions.

4.2 *Detection of Defects in Field Conditions*

Another application is the detection of defects during the inspection of composite structures in field conditions. For this purpose, the system was used in the testing area of a major aeronautical manufacturer on reference structures with known induced defects. Figure 8(a) shows the instrument observing a part of a large composite structure with a zone where a series of induced known defects are present. Figure. 8(b) and 8(c) shows phase maps of such defective areas after thermal loading has been applied by halogen lamps. Defects (surrounded in red) clearly appear as local differential patterns. The structure shown in Fig. 8(a) was sprayed with the removable white powder because the convex shape prevented homogeneous scattered speckle pattern from being obtained on the camera.

The large structure inspected was placed in a hangar with people working around it and a lot of engines running in the background. Moreover, the hangar doors were opened so external air could enter the hangar. Such working conditions would prevent the use of such an ESPI method if it were applied with VIS wavelengths.

5 Discussion and Conclusions

In this paper, we have shown the development of a mobile instrument based on ESPI in the LWIR range, which uses a CO_2 laser and a thermal infrared camera based on the uncooled microbolometer array technology. The optical head of the system incorporated all the necessary components, such as the laser, the camera, and various optical

and optomechanical devices. It can be transported on measurement sites, and it was used in various industrial applications for demonstrating the ability to use such long-wavelength interferometers to work in perturbed environments. The instrument was used for monitoring out-of-plane deformations of a composite panel in tensile testing and in the case of a long helicopter tailboom in a testing rig with a hydraulic actuator. Additionally, it was used to detect defects in a large aircraft composite structure in a normal inspection area of a hangar. However, the system is more complicated and expensive than the shearography technique.[18] The results presented are of a similar quality as those usually obtained with VIS ESPI. Since the laser wavelength used is 20 times larger than in VIS, the measurement range is also 20 times larger. The other advantage is that sensitivity to external perturbations is decreased by the same factor. This technique fills a gap between VIS holographic/speckle interferometry techniques and other techniques based on imagery, like fringe projection and videogrammetry, which are much less sensitive to displacements, as already pointed out in our previous paper.[16]

Acknowledgments

These works are funded by the FP7 European project FANTOM (ACP7-GA-2008-213457). Different entities participated in the project: the different holographic and speckle techniques were studied by both the Centre Spatial de Liège and the Institut für Technische Optik, with the support of Infratec GmbH, which is a leading EU-based company in the development of thermography equipment. Optrion S.A. was in charge of the building of mobile unit, whereas the Centro de Tecnologias Aeronáuticas was active in qualifying the system in industrial environments.

References

1. C. M. Vest, *Holographic Interferometry*, Wiley & Sons, New York (1979).
2. R. Jones and C. Wykes, *Holographic and Speckle Interferometry*, Cambridge University Press, Cambridge, United Kingdom (1989).
3. M. P. Georges et al., "Digital holographic interferometry with CO_2 lasers and diffuse illumination applied to large space reflector metrology," *Appl. Opt.* **52**(1), A102–A116 (2013).
4. O. J. Løkberg and O. Kwon, "Electronic speckle pattern interferometry using a CO_2 laser," *Opt. Laser Technol.* **16**(4), 187–192 (1984).
5. E. Allaria et al., "Digital holography at 10.6 μm," *Opt. Commun.* **215**(4–6), 257–262 (2003).
6. S. De Nicola et al., "Infrared digital reflective-holographic 3D shape measurements," *Opt. Commun.* **281**(6), 1445–1449 (2008).
7. N. George, K. Khare, and W. Chi, "Infrared holography using a microbolometer array," *Appl. Opt.* **47**(4), A7–A12 (2008).
8. M. Paturzo et al., "Optical reconstruction of digital holograms recorded at 10.6 μm: route for 3D imaging at long infrared wavelengths," *Opt. Lett.* **35**(12), 2112–2114 (2010).
9. A. Geltrude et al., "Infrared digital holography for large objects investigation," *Proc. SPIE* **8082**, 80820C (2011).
10. A. Pelagotti et al., "Digital holography for 3D imaging and display in the IR range: challenges and opportunities," *3D Res.* **1**, 6 (2011).
11. J.-F. Vandenrijt and M. Georges, "Infrared electronic speckle pattern interferometry at 10 μm," *Proc. SPIE* **6616**, 66162Q (2007).
12. J.-F. Vandenrijt and M. Georges, "Electronic speckle pattern interferometry with microbolometer arrays at 10.6 μm," *Appl. Opt.* **49**(27), 5067–5075 (2010).
13. I. Yamaguchi, "Fundamentals and applications of speckle," *Proc. SPIE* **4933**, 1–8 (2003).
14. J.-F. Vandenrijt et al., "Electronic speckle pattern interferometry at long infrared wavelengths. Scattering requirements," in *Fringe 2009—6th International Workshop on Advanced Optical Metrology*, W. Osten and M. Kujawinska, Eds, pp. 1–4, Springer-Verlag, Berlin, Heidelberg (2009).
15. I. Alexeenko et al., "Digital holographic interferometry by using long wave infrared radiation (CO_2 laser)," *Appl. Mech. Mater.* **24–25**, 147–152 (2010).
16. I. Alexeenko et al., "Nondestructive testing by using long-wave infrared interferometric techniques with CO_2 lasers and microbolometer arrays," *Appl. Opt.* **52**(1), A56–A67 (2013).
17. N. Diakides and J. Bronzino, *Medical Thermal Imaging*, CRC Press, Boca Raton, Florida (2007).
18. M. Kalms and W. Osten, "Mobile shearography system for the inspection of aircraft and automotive components," *Opt. Eng.* **42**(5), 1188–1196 (2003).

Jean-François Vandenrijt received a PhD in engineering from the University of Liège (Belgium) in 2010. He is currently working as an optical engineer at the Centre Spatial de Liège (CSL), a space research center of the University of Liège, in the Laser and NDT Laboratory. His research focuses on the development of optical metrological instruments in the visible and thermal infrared spectrum, with applications in NDT for the aeronautic and space industries, and optical metrology for measuring the deformation of large-space reflectors in thermal vacuum conditions.

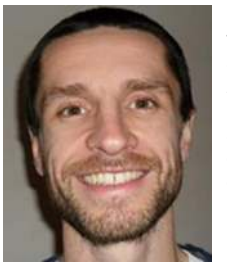

Cédric Thizy received an MS in optoelectronics from the Queen's University of Belfast and then joined the Centre Spatial de Liège in 2000, where he has been working on several Belgian, European, and ESA projects ever since. His research activities are in the areas of holographic interferometry, optical metrology, and NDT. He is the author or coauthor of more than 50 papers.

Igor Alexeenko received the master in physics (specialization in radiophysics) in 1995 and the doctor degree in radiophysics in 2006 from the Kaliningrad State University (Russia). After completing post-doctoral stay at the Institute für Technische Optik at the University of Stuttgart, he is currently working as researcher at laboratory of optical measuring systems at Immanuil Kant Federal University (Kaliningrad). His activity includes investigations in digital holography, digital holographic interferometry in wide spectral range and measuring of dynamic processes by optical methods and NDT.

Giancarlo Pedrini received his MS in physics from the Swiss Federal Institute of Technology (ETH-Zurich) in 1982 and his PhD in optical sciences from the University of Neuchatel (Switzerland) in 1990. He joined the Institut für Technische Optik at the University of Stuttgart in 1991. His research areas include digital holography, vibration analysis, shape measurement, optical testing, measurement of the elastic parameters of biological samples, endoscopy, and phase retrieval.

Jonathan Rochet earned an optoelectronics engineering degree in 2006 from Paris XI University (U-psud). He is working as a business development manager at Optrion, a Belgian spin-off of the CSL dedicated to the development and industrialization of industrial holographic systems used in NDT. He is currently working on the development of a shearography NDT system in partnership with an industrial end user.

Birgit Vollheim received her BS degree in electrical engineering in 1983 and obtained a PhD (Dr-Ing) in 1992, both from the Dresden University of Technology (Germany). Until 1991, she worked as an R&D engineer on the design of read-out integrated circuits for IR detector arrays. As a senior scientist at the Institute of Solid-State Electronics at the Dresden University of Technology, she was later involved in several research projects concerning the application and development of infrared cameras. Since 2004, she has been involved in the R&D department of InfraTec GmbH Dresden, where she is dealing with the development and radiometric calibration of thermographic cameras, focusing particularly on the evaluation of appropriate infrared detectors and optical add-ons.

Iagoba Jorge received his BS in industrial engineering in 2007 from the Faculty of Engineering. of Logroño (Spain) and was graduated in 2012 as a master in space science and technology from the Faculty of Engineering of the University of the Basque Country in Bilbao (Spain). Now he is performing investigations leading to PhD degree at the University of the Basque Country. He has been working as project manager at CTA (Aeronautical Technologies Centre) since 2008, participating in different R&D (Infrared Thermography and Avionics) projects for aeronautical sector. He has been involved in several structural test projects related with different aircraft models (Airbus A320, A 350, A380, and A400M). In the beginning of 2013 he has become Responsible of Avionics area at The Aeronautical Technologies Centre. His main research domain is Structural Health Monitoring (including sensor development and certification).

Pablo Venegas obtained his BS degree in industrial engineering in 2006 at the Faculty of Engineering of the University of the Basque Country and has more than 6 years of experience in the aeronautical sector in the research and development of thermographic techniques applied as NDT tools. He has a master's degree in investigation in industrial technologies obtained at the UNED University and is now a PhD student. He has been working in The Aeronautical Technologies Centre as a project manager for more than 6 years, where has gained experience in national and European projects in the investigation of the thermographic technology as well as in the evaluation and validation of new NDT techniques. In the beginning of 2013 he has become Responsible of NDT area in The Aeronautical Technologies Centre.

Ion López received his BS in industrial engineering in 2002 from the Faculty of Engineering of the Basque Country (Bilbao) He is PhD student at the University of Cantabria. He has been working as head of Singular Projects at CTA (Aeronautical Technologies Centre) since 2008, participating in different certification test campaign for aeronautical sector and different R&D projects. He has been involved as project manager in several structural test projects related with different aircraft models (A320, A340, A380, and A400M). His main research domains are combustion and scale model fire tests and infrared thermography as NDT technique for defect detection.

Wolfgang Osten received the diploma in physics from the Friedrich-Schiller-University Jena in 1979 and in 1983 the PhD degree from the Martin-Luther-University Halle-Wittenberg for his thesis in the field of holographic interferometry. From 1984 to 1991, he was employed at the Central Institute of Cybernetics and Information Processes in Berlin making investigations in digital image processing and computer vision. In 1991, he joined the Bremen Institute of Applied Beam Technology (BIAS) to establish the Department Optical 3D-Metrology. Since September 2002, he has been a full professor at the University of Stuttgart and director of the Institute for Applied Optics. His research work is focused on new concepts for industrial inspection and metrology by combining modern principles of optical metrology, sensor technology, and image processing. Special attention is directed to the development of resolution enhanced technologies for the investigation of micro and nano structures.

Marc P. Georges obtained his license in physics at the Université Catholique de Louvain (Belgium) in 1989 and his D.E.A. in physics from the same university in 1990. He joined the CSL in 1990, where he developed holographic instruments based on photorefractive crystals for metrology, vibration analysis, and defect detection in the frame of his PhD thesis, obtained in 1998. Since then, he has led various projects on holographic metrology for industry and aerospace applications. Since 2006, he has been responsible of the Laser and NDT Laboratory at CSL. He initiated several projects in the field of holographic metrology in the far infrared spectrum and is the coordinator of EU and ESA projects on this topic. His current interest is NDT of composites, with ongoing development of full-field techniques, including shearography, thermography, and laser ultrasonics.